



## A new device for *in situ* static and dynamic calibration of force platforms

Hong-Jung Hsieh<sup>a,c,1</sup>, Tung-Wu Lu<sup>b,1,\*</sup>, Sheng-Chang Chen<sup>b</sup>, Chia-Min Chang<sup>b</sup>, Chinghua Hung<sup>a</sup>

<sup>a</sup> Institute of Mechanical Engineering, National Chiao-Tung University, Taipei, Taiwan, ROC

<sup>b</sup> Institute of Biomedical Engineering, National Taiwan University, Taiwan, ROC

<sup>c</sup> Department of Mechanical and Automation Engineering, Kao-Yuan University, Taiwan, ROC

### ARTICLE INFO

#### Article history:

Received 15 May 2010

Received in revised form 17 February 2011

Accepted 7 March 2011

#### Keywords:

Motion analysis

Force plate

Calibration

Center of pressure

### ABSTRACT

In human motion analysis, *in situ* calibration of the force plate is necessary to improve the accuracy of the measured ground reaction force (GRF) and center of pressure (COP). Few existing devices are capable of both static and dynamic calibration of the usually non-linear GRF and COP errors, while are also easy to move and/or set up without damaging the building. The current study developed a small device (160 cm × 88 cm × 43 cm) with a mass of 50 kg, equipped with auxiliary wheels and fixing suction pads for rapid deployment and easy set-up. A PC-based controller enabled quick movement and accurate positioning of the applied force to the calibration point. Static calibration at 100 validation points and dynamic calibration of a force plate were performed using the device. After correction by an artificial neural network (ANN) trained with the static data from another 121 points, the mean errors for the GRF were all reduced from a maximum of 0.64% to less than 0.01%, while those for the COP were all reduced from a maximum of about 1.37 mm to less than 0.04 mm. For dynamic calibration, the mean errors for the GRF were reduced from a maximum of 0.46% to less than 0.28%, while those for the COP were reduced from a maximum of 0.95 mm to less than 0.11 mm. The results suggest that the calibration device with the ANN method will be useful for obtaining more accurate GRF and COP measurements in human motion analysis.

© 2011 Elsevier B.V. All rights reserved.

### 1. Introduction

Gait analysis has been widely used in the diagnosis of neuromusculoskeletal pathology and the assessment of the outcome of subsequent treatment [1–7]. Generally, kinematic and force plate data are necessary for computing the joint forces, moments and powers using inverse dynamics techniques [8–10]. Apart from the measured kinematic data, it has been shown that the accuracy of the ground reaction forces (GRF) and the center of pressure (COP) measured by the force plate has a significant impact on the calculated joint kinetics [11–13]. Since inaccuracies of the force plate mounted flush with the floor may occur as a result of improper installation, aging, or other damages [14,15], *in situ* calibration is required to ensure the accuracy of the measurements, and thus the gait analysis results.

Several calibration devices for *in situ* calibration of force plates have been described in the literature [16–19]. Bobbert and Schamhardt designed a calibration device to apply static vertical forces at 117 calibration points to quantify the measured COP errors that were then corrected using polynomial regression

equations. Dynamic calibration was performed only for COP but not GRF. Hall et al. [18] performed a static vertical and horizontal force calibration using a point loader and a pulley rig, and cross-sensitivity matrices were obtained for correcting errors in the measured forces and COP positions. It is noted that both devices required extensive structural changes to the laboratory building and did not allow dynamic force calibration. To overcome the problem of damage to the floor, Gill and O'Connor [17] designed a device (mass: 400 kg; volume: 1.71 m × 1.54 m × 0.8 m) which enabled the application of known static vertical forces at several calibration points using a manually controlled lever system, making it difficult to ensure the accuracy and speed of positioning. The correction of measurement errors was not described. Collins et al. reported a linear, least-squares calibration method for force plates and treadmills using data from arbitrary calibration points [20] but only static calibration was performed for the force plate. Goldberg et al. increased the accuracy of an instrumented treadmill's measurement of center of pressure and force data by calibrating statically the transformation between the coordinate systems motion capture and treadmill force plate [21].

Until now, few existing devices are capable of both static and dynamic calibration of GRF and COP errors with high positioning accuracy, while are also easy to move and/or set up without damaging the building. Since there is a significant correlation between measured forces and COP positions that are also non-

\* Corresponding author. Tel.: +886 233 653 335; fax: +886 233 653 335.

E-mail address: [twlu@ntu.edu.tw](mailto:twlu@ntu.edu.tw) (T.-W. Lu).

<sup>1</sup> These authors contributed equally to this work.

linear across the force plate [16,17], using linear cross-sensitivity matrices for error correction is restricted. A correction procedure considering the coupling and non-linear nature of the GRF and COP is necessary for accurate force plate measurements. The purposes of this study were to build a new *in situ* force plate calibration device that has the above-mentioned features, and to develop a correction method based on an artificial neural network (ANN) for correcting the measured force plate data.

## 2. Materials and methods

### 2.1. Calibration device

The current calibration device uses the principle of leverage to control the magnitudes and positions of the forces applied to the force plate under test. The device consists of a base secured to the floor by eight industrial suction pads, an arm that rotates about and moves along an axis relative to the base, a loading rod that moves along the arm, and a carrier that carries calibrating weights and moves along the arm on a ball screw, Fig. 1. A ball bearing of 15 mm diameter at the end of the loading rod was used to transmit the load to the force plate. The suction pads were used to counter-balance the forces applied to the force plate, whereas previous devices achieved this by fixing themselves to the floor [16,18] or by their weights [17]. This design significantly reduced the weight and volume of the device (mass: 50 kg; volume: 160 cm × 88 cm × 43 cm) and thus enabled rapid mounting without damaging the floor. For accurate positioning of a calibration point, each moving axis of the device was driven by a step motor and controlled by a PC-based controller, and measured using encoders with an accuracy of 0.00125 mm.

For a given calibration point, the force applied to the force plate is determined by considering moment equilibrium at the base axis as follows (Fig. 1):

$$R = \frac{Wl + W_a l_a + W_p d}{d} \quad (1)$$

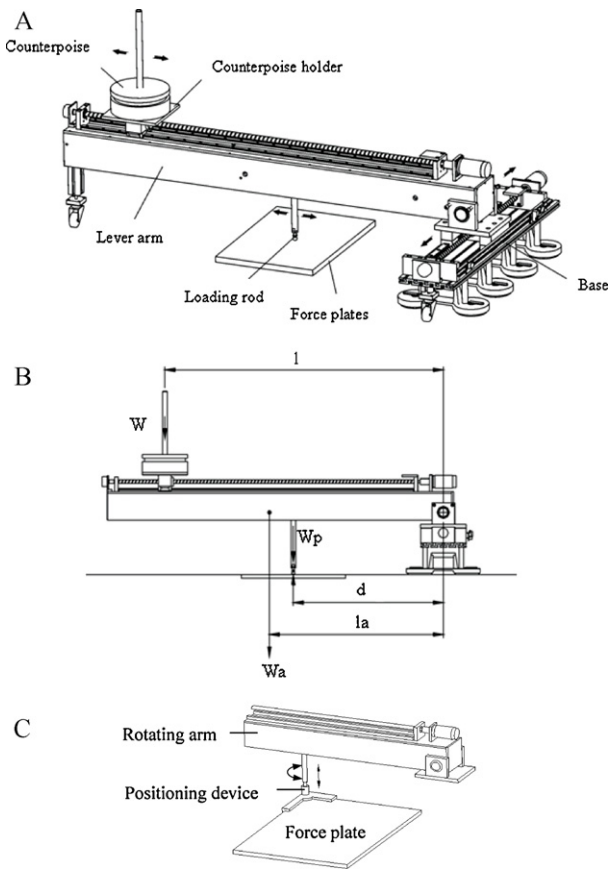


**Fig. 1.** (A) Setup of the device for calibrating a force plate. (B) Force diagram showing the determination of the calibration loads ( $W_p$ ) from the weight of the counterpoise ( $W$ ), the weight of the lever-arm ( $W_a$ ) and their respective positions  $d$ ,  $l$  and  $l_a$ . The wheel at the left endpoint of the lever-arm did not touch the floor during force plate calibration. (C) A height-adjustable positioning device with its two L-shaped legs aligned with the two edges of a corner of the force plate for the definition of the position of the corner.

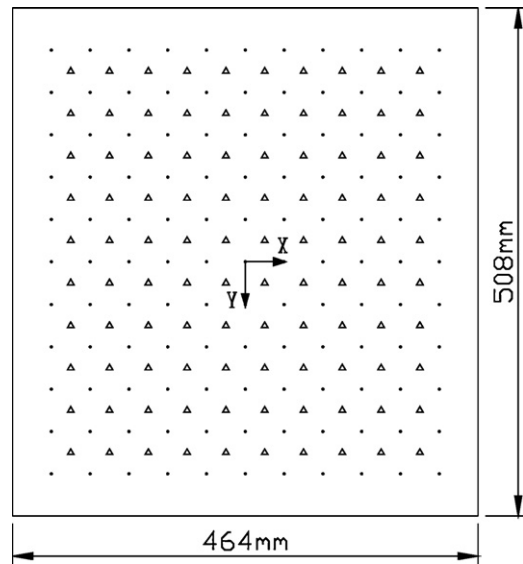


**Fig. 2.** The positions of 121 calibration points (dot) and 100 validation points (triangle) on the force plate.

where  $R$  is the GRF;  $W$  is the calibration weight;  $W_p$  is the weight of the loading rod (17.07 N); and  $W_a$  is the weight of the rotating arm, with lever-arm lengths of  $l$  and  $l_a$ , respectively. All lever-arm lengths were measured by encoders, while the force plate data were collected simultaneously through an A/D converter at a sampling rate of 120 Hz (National Instruments, USA). The accuracy of the calibration load was less than 0.007 N, estimated experimentally using a load-cell (capacity 2000 N; precision 0.0045 N; Sensotec Inc., USA).

### 2.2. Static calibration tests

A force plate (OR6-7-1000, AMTI, USA) was tested by the calibration device that was positioned next to the force plate with the rotating arm parallel to its short edge. The coordinates of the four corners of the force plate were digitized five times using a positioning device based on the load rod (Fig. 2), and the averaged coordinates used for determining the coordinate transformations between the calibration device and force plate. The calibration system then generated a grid of 121 calibration points (Fig. 2). At each point, vertical loads of 650 N, 800 N and 1000 N were applied while the measured forces and moments, and COP were collected at a sampling rate of 120 Hz for two seconds. Data were also obtained for another grid of 100 validation points (Fig. 2).

### 2.3. Dynamic calibration tests

Dynamic calibration was performed at the center of the force plate. The dynamic loading history was created by moving a 20 kgf weight on the counterpoise holder forward and backward over a range of 100 cm at speeds of 7.5 cm/s and 25.0 cm/s, with the applied force varying linearly between 987 and 523 N. This enabled the calibration of not only the COP position, but also the loading values under dynamic conditions. For calibration of COP position at higher dynamic loads, a young subject with a body mass of 60 kg was asked to stand with one leg on the counterpoise holder, and the other on a platform with the same height placed outside the force plate. By shifting from two-leg stance to single-leg stance on the counterpoise holder, the dynamic condition during walking could be simulated. This type of dynamic calibration was performed at three different counterpoise holder positions, to simulate three vertical loading ranges, namely 800–1400 N, 650–800 N and 450–650 N. Owing to the problems with the calculated COP positions under small vertical forces during initial and terminal ground contact [14,16], only the data within the three force ranges were used for quantifying the mean and standard deviation of the errors in the COP position. The forces and moments measured by the force plate were collected at a sampling rate of 1000 Hz.

### 2.4. Calculation of COP position

The COP position was described relative to the force plate coordinate system, originating at the geometric center of the plate, with the X-axis along the short edge and the Y-axis along the long edge (Fig. 1). Given the measured forces  $\mathbf{F} = (F_x, F_y, F_z)$  and moments  $\mathbf{M} = (M_x, M_y, M_z)$  about the origin, the COP position  $\mathbf{P} = (P_x, P_y, P_z)$  was calculated as follows:

$$P_x = \frac{P_z F_x - M_y}{F_z} \quad (2)$$

$$P_y = \frac{M_x + P_z F_y}{F_z} \quad (3)$$

### 2.5. ANN-based correction method

For correction of force plate measurement errors, a four-layered, fully connected, feed-forward, back-propagation ANN [22] was constructed, with 5 neurons each in the input and output layers, 10 in the first hidden layer, and 8 in the second. A bias of  $-1$  was added to each of the neurons in the first and second hidden layers, with a transfer function of  $\tanh(x)$ . This structure was determined empirically. The ANN was trained to learn the relationship between the measured (input) and true (output) forces ( $F_x, F_y, F_z$ ) and COP positions ( $P_x, P_y$ ) using data of the 121 calibration points through an optimization procedure based on the BFGS algorithm and golden section line search. The training stopped when the norm of the difference between the predicted and targeted outputs is less than  $1 \times 10^{-15}$ . The trained ANN was then used to correct errors for the 100 validation points and data in the dynamic tests.

### 2.6. Statistical analysis

In the static calibration, the differences between the given and measured GRF and COP positions (i.e. measurement errors) were averaged across the 100 validation points, giving their means, standard deviations, and minimum and maximum values. In the dynamic calibration with given loads at the force plate center, the errors of the GRF and COP positions were time-averaged to give means and standard deviations. In the dynamic calibration of COP position at higher dynamic load, the time-averaged means and standard deviations of the COP errors were also calculated. All these calculations were performed both before and after ANN correction.

## 3. Results

### 3.1. Static calibration

The errors in the GRF and COP were smallest around the center of the force plate and increased with increased distance from the center, Fig. 3(A and C). The ensemble-averaged percent errors of

the measured  $F_z$  over the 100 validation points under three static calibration loads ranged from 0.30% to 0.32%, Table 1. The corresponding values were  $-0.32$  and  $-0.28\%$  for  $F_x$ , and  $0.58\%$  and  $0.64\%$  for  $F_y$ , indicating small cross-talks with  $F_z$ . The maximum and minimum errors of the forces were  $1.67\%$  and  $-1.84\%$ , respectively, and became  $-0.5\%$  to  $0.33\%$  after ANN correction. Mean errors in  $P_x$  ranged from  $1.32$  to  $1.33$  mm, while those for  $P_y$  ranged from  $1.05$  to  $1.08$  mm, Table 1. The maximum and minimum errors of  $P_x$  and  $P_y$  were  $-2.14$  and  $2.97$  mm, respectively, and became  $-0.36$  and  $1.26$  mm after ANN correction. The mean error at the center of the plate was  $-0.46$  mm for  $P_x$  and  $0.81$  mm for  $P_y$ . After correction using the ANN, the mean errors in the three GRF components were all reduced to less than  $0.01\%$ , while those in the COP were all less than  $0.04$  mm, Table 1. This shows that the ANN successfully corrected the non-linear GRF and COP errors across the force plate, Fig. 3(B and D).

### 3.2. Dynamic calibration with given forces at force plate center

During calibration at the center of the force plate under forces at two loading rates, the mean errors in measured  $F_z$  were between  $-0.16\%$  and  $-0.19\%$  (Table 2). The corresponding values for  $F_x$  were  $-0.51\%$  and  $-0.46\%$ , and  $0.37\%$  and  $0.39\%$  for  $F_y$ . After ANN correction, the mean errors were reduced to a range between  $-0.03\%$  and  $-0.01\%$  for  $F_z$ , and  $-0.28\%$  and  $-0.2\%$  for  $F_x$  and  $F_y$ . However, the standard deviations were not significantly decreased. The mean errors and standard deviations in the measured COP positions did not appear to be affected by loading rates, the mean errors in  $P_x$  being between  $-0.53$  and  $-0.5$  mm, and those in  $P_y$  between  $0.9$  and  $0.95$  mm, Table 2. Compared to the COP positions measured during static calibration, the mean errors in  $P_x$

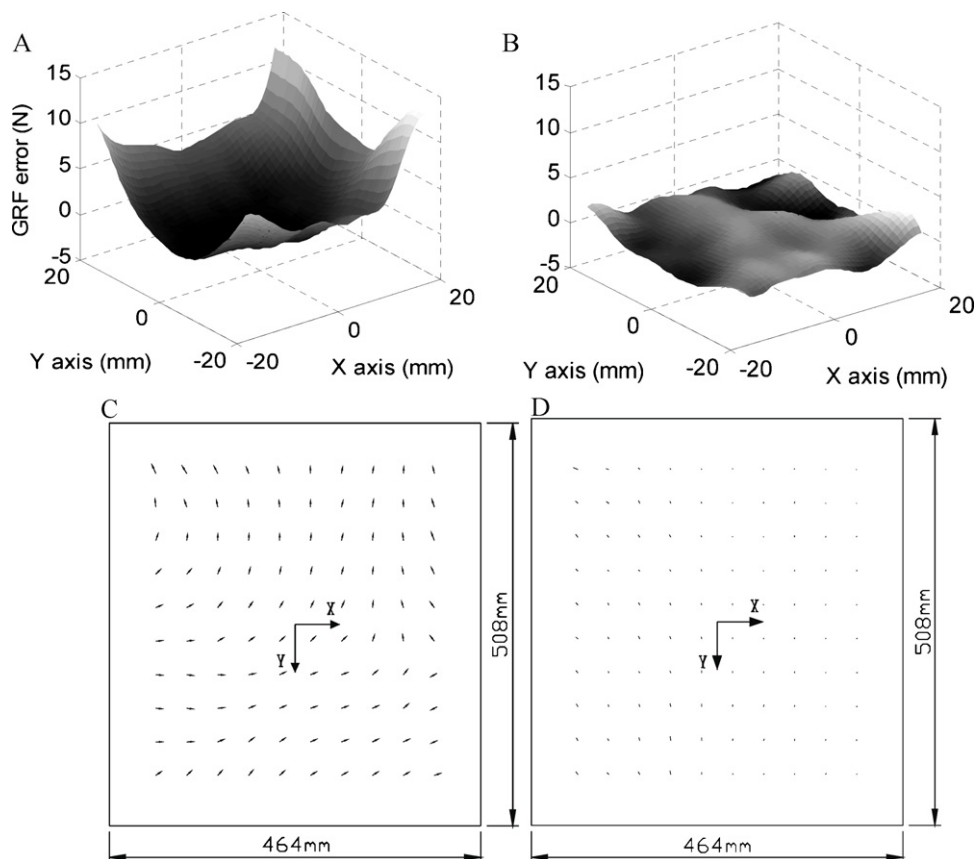


**Fig. 3.** Mean errors in the GRF at each of the 100 validation points, under a static calibration load of 1000 N (A) before and (B) after ANN correction, and vectors of mean COP errors at each of the 100 validation points under a static calibration load of 1000 N (C) before and (D) after ANN correction. The vectors are drawn to a scale of five times the actual scale.

**Table 1**  
Means (standard deviations, SD) and ranges (minimum and maximum value) of percent errors in the measured GRF, and errors in the COP over the 100 validation points under three static calibration loads before and after ANN correction.

Errors		Vertical loads (N)					
		650		800		1000	
		Before	ANN	Before	ANN	Before	ANN
$F_x$ (%)	Mean (SD)	-0.28 (0.20)	0.01 (0.09)	-0.31 (0.21)	0.01 (0.13)	-0.32 (0.20)	0.00 (0.07)
	Min, Max	-0.73, 0.08	-0.15, 0.21	-0.75, 0.05	-0.13, 0.21	-0.75, 0.05	-0.13, 0.21
$F_y$ (%)	Mean (SD)	0.64 (0.18)	0.01 (0.07)	0.61 (0.17)	-0.01 (0.07)	0.59 (0.16)	0.01 (0.07)
	Min, Max	0.32, 0.98	-0.17, 0.14	0.30, 0.96	-0.17, 0.12	0.30, 0.96	-0.17, 0.12
$F_z$ (%)	Mean (SD)	0.38 (0.48)	0.01 (0.19)	0.39 (0.47)	0.00 (0.14)	0.41 (0.44)	0.00 (0.13)
	Min, Max	-1.84, 1.67	-0.50, 0.33	-0.28, 1.53	-0.27, 0.26	-0.28, 1.53	-0.27, 0.26
$P_x$ (mm)	Mean (SD)	1.33 (0.78)	0.03 (0.23)	1.32 (0.75)	0.03 (0.24)	1.32 (0.74)	0.02 (0.23)
	Min, Max	-2.14, 1.77	-0.35, 0.92	-2.14, 1.77	-0.33, 0.96	-2.03, 1.66	-0.36, 0.86
$P_y$ (mm)	Mean (SD)	1.08 (0.70)	0.04 (0.24)	1.07 (0.73)	0.03 (0.23)	1.05 (0.75)	0.03 (0.24)
	Min, Max	-0.41, 2.97	-0.23, 1.16	-0.41, 2.97	-0.19, 1.26	-0.53, 2.97	-0.21, 1.10

Min: minimum value.

Max: maximum value.

during dynamic calibration were between  $-0.11$  and  $-0.04$  mm, while those in  $P_y$  were between  $0.08$  and  $0.14$  mm. After ANN correction, the mean errors in  $P_x$  were reduced to between  $-0.01$  and  $0.03$  mm, and those in  $P_y$  were between  $-0.11$  and  $-0.05$  mm. Therefore, it appeared that the ANN trained by static calibration data was effective in correcting the COP errors for dynamic loadings (Table 2).

### 3.3. Dynamic calibration of COP with unknown dynamic loading

Under different dynamic loads at the given position, the mean errors in  $P_x$  and  $P_y$  were  $-0.7$  mm and  $0.9$  mm, respectively, with standard deviations of  $0.72$  and  $0.71$  mm. After ANN correction, the mean errors in  $P_x$  and  $P_y$  were reduced to  $-0.1$  and  $0.15$  mm, respectively, with standard deviations of  $0.73$  and  $0.68$  mm.

## 4. Discussion

The current study aimed to design and build a new device for *in situ* static and dynamic calibration of a force plate. In contrast to previous designs described in the literature, the current device was light-weight, portable, and easy to set up without causing damage to the laboratory building. It also enabled simple, quick and accurate positioning of forces. An ANN trained with static calibration data was shown to be effective in correcting non-linear errors, both in force magnitudes and COP positions, during static and dynamic calibration tests. The device and the associated ANN are considered useful for calibrating force plates for motion analysis.

The weight of a calibration device, its stability and the time required to set it up are crucial for the *in situ* calibration of a force

**Table 2**  
Means (standard deviations, SD) of percent errors in the measured GRF and errors in the COP at the center of the force plate under linear dynamic loading by moving the weight (20 kgf) at speeds of  $7.5$  and  $25$  cm/s before and after ANN correction.

	Moving velocity of the weight (cm/s)			
	7.5		25	
	Before	ANN	Before	ANN
$F_x$ (%)	-0.46 (0.12)	-0.23 (0.11)	-0.51 (0.12)	-0.28 (0.11)
$F_y$ (%)	0.39 (0.07)	-0.2 (0.08)	0.37 (0.08)	-0.21 (0.08)
$F_z$ (%)	-0.19 (0.72)	-0.03 (0.72)	-0.16 (1.30)	-0.01 (1.30)
$P_x$ (mm)	-0.50 (0.67)	-0.01 (0.69)	-0.53 (0.68)	0.03 (0.69)
$P_y$ (mm)	0.95 (0.90)	-0.11 (0.59)	0.90 (0.64)	-0.05 (0.65)

plate. Because of the requisite stability, some designs rely on the weight and dimensions of the device [17,18], while others have to be fixed to the laboratory building, causing intrusive damage to the building [18]. Both approaches require a lot of time and effort to set up the device. In the current study, the device had a mass of  $50$  kg with a small size ( $160$  cm  $\times$   $88$  cm  $\times$   $43$  cm) and was equipped with auxiliary wheels and fixing suction pads, making it easy to deploy. On average, the new calibration device could be set up within  $10$  min by two people, which is acceptable for regular *in situ* calibration of force plates in motion analysis laboratories.

Accuracy of the calibrating forces and the points of application applied by the calibration device to the force plate is important for accurate calibration of the force plate. In previous studies, the point of application of the calibrating force was defined by marking it on the surface of the force plate, and the force-applying component was then moved manually onto the calibration point [16–18]. This process was slow and cumbersome, and was subject to positioning errors. In contrast, the current device had a PC-based controller to manipulate the lever-arm for quick and accurate positioning of the loading rod to the calibration point. This capability also enabled rapid definition of the coordinate system of the device, and the calibration of  $121$  points under any load within  $30$  min as opposed to at least  $1$  h for devices mentioned in the literature [17].

The major factor affecting the accuracy of the measured GRF and COP appeared to be the location of the applied force. The errors in the measured GRF and COP were non-linear across the force plate, those around the center being the smallest, Fig. 2. The errors in the COP at a calibration point appeared to be less affected by the applied force. Similar results were also found in previous studies [16,17]. Without error correction, the subject would have to step as close as possible to the center of the force plate to reduce the errors of measurements, thereby reducing the effective area of measurement. This may increase the time required for the gait test and become a problem when the subject has difficulty in doing so while maintaining his/her natural movement pattern. This problem can be resolved with the proposed ANN technique because non-linear errors can be successfully corrected (Fig. 2B and D, Table 1).

Using the current calibration device, the errors in the GRF and COP under dynamic calibration with given COP and forces did not seem to be affected by loading speeds under  $25$  cm/s. These errors were significantly decreased after correction using the ANN trained with static calibration data (Table 2). On the other hand, dynamic calibration with unknown loading at given COP showed that the errors in the COP under high loading speed were greater than those under a speed of  $25$  cm/s. This suggests that the errors

in COP were affected by the loading velocity although they could be corrected to a certain extent by the ANN trained with static data. Further study is needed to investigate whether inclusion of dynamic calibration data in the training of the ANN would help improve the efficacy of error correction.

The use of ANN for error correction seemed to be a good choice because the errors in the measured COP, GRF and loading speed were inter-related and were non-linear across the force plate. The ANN is very powerful for mapping highly non-linear inputs and outputs in multiple dimensions. Bobbert and Schamhardt were able to use a quadratic formula to correct the COP errors for a Kistler force plate because the COP errors were generally symmetric with respect to the force plate center [16]. The effect of loading magnitude and speed on the COP errors were not considered. For the current force plate, the error distribution of the COP was not symmetrical. Similar results were also found by Gill and O'Connor [17]. Therefore, a symmetrical formula would not be sufficient for error correction. Hall et al. used linear cross-sensitivity matrices based on data from a small number of calibration points for error correction [18]. With the non-linear nature of the error distribution across the current force plate, however, this approach is expected to produce non-linear residual errors. The current ANN approach does not assume symmetric or linear distribution of the errors, and has been shown to correct the measured non-linear errors in the GRF and COP successfully. Therefore, incorporating the ANN method into a calibration procedure based on the calibration device will be useful for more accurate GRF and COP measurements using a force plate.

## 5. Conclusions

A new *in situ* calibration device was developed for static and dynamic calibration of a force plate. The device was light-weight, portable, and easy to set up without causing damage to the laboratory building. The device also enabled simple, quick and accurate positioning of applied forces. An ANN trained with static calibration data was shown to be effective in correcting errors, both in force magnitudes and COP positions, during static and dynamic calibration tests. The new calibration device with the ANN method will be useful for more accurate GRF and COP measurements in human motion analysis.

## Conflict of interest statement

The authors, declare that they have no proprietary, financial, professional or other personal interest of any nature or kind in any product, service and/or company that could be construed as

influencing the position presented in, or the view of, this manuscript.

## References

- [1] Liu MW, Hsu WC, Lu TW, Chen HL, Liu HC. Patients with type II diabetes mellitus display reduced toe-obstacle clearance with altered gait patterns during obstacle-crossing. *Gait Posture* 2010;31(1):93–9.
- [2] Huang SC, Wei IP, Chien HL, Wang TM, Liu YH, Chen HL, et al. Effects of severity of degeneration on gait patterns in patients with medial knee osteoarthritis. *Med Eng Phys* 2008;30(8):997–1003.
- [3] Lu TW, Chen HL, Wang TM. Obstacle crossing in older adults with medial compartment knee osteoarthritis. *Gait Posture* 2007;26(4):553–9.
- [4] Crenshaw SJ, Pollo FE, Calton EF. Effects of lateral-wedged insoles on kinetics at the knee. *Clin Orthop Relat Res* 2000;375:185–92.
- [5] Powers CM, Heino JG, Rao S, Perry J. The influence of patellofemoral pain on lower limb loading during gait. *Clin Biomech (Bristol Avon)* 1999;14(10):722–8.
- [6] Goh JC, Bose K, Khoo BC. Gait analysis study on patients with varus osteoarthritis of the knee. *Clin Orthop Relat Res* 1993;294:223–31.
- [7] Messier SP, Loeser RF, Hoover JL, Semble EL, Wise CM. Osteoarthritis of the knee—effects on gait, strength, and flexibility. *Arch Phys Med Rehab* 1992;73(1):29–36.
- [8] Inman VT, Ralston HJ, Todd F. *Human walking*. Baltimore: Williams & Wilkins; 1981.
- [9] Bresler B, Frankel JP. The forces and moments in the leg during level walking. *Trans ASME* 1950;72(1):27–36.
- [10] Elftman H. Forces and energy changes in the leg during walking. *Am J Physiol* 1939;125(2):339–56.
- [11] Cappozzo A, Leo T, Pedotti A. A general computing method for the analysis of human locomotion. *J Biomech* 1975;8(5):307–20.
- [12] Koopman B, Grootenboer HJ, de Jongh HJ. An inverse dynamics model for the analysis, reconstruction and prediction of bipedal walking. *J Biomech* 1995;28(11):1369–76.
- [13] McCaw ST, DeVita P. Errors in alignment of center of pressure and foot coordinates affect predicted lower extremity torques. *J Biomech* 1995;28(8):985–8.
- [14] Chockalingam N, Giakas G, Iossifidou A. Do strain gauge force platforms need *in situ* correction? *Gait Posture* 2002;16(3):233–7.
- [15] Schmiedmayer HB, Kastner J. Parameters influencing the accuracy of the point of force application determined with piezoelectric force plates. *J Biomech* 1999;32(11):1237–42.
- [16] Bobbert MF, Schamhardt HC. Accuracy of determining the point of force application with piezoelectric force plates. *J Biomech* 1990;23(7):705–10.
- [17] Gill HS, O'Connor JJ. A new testing rig for force platform calibration and accuracy tests. *Gait Posture* 1997;5(3):228–32.
- [18] Hall MG, Fleming HE, Dolan MJ, Millbank SF, Paul JP. Static *in situ* calibration of force plates. *J Biomech* 1996;29(5):659–65.
- [19] Middleton J, Sinclair P, Patton R. Accuracy of centre of pressure measurement using a piezoelectric force platform. *Clin Biomech (Bristol Avon)* 1999;14(5):357–60.
- [20] Collins SH, Adamczyk PG, Ferris DP, Kuo AD. A simple method for calibrating force plates and force treadmills using an instrumented pole. *Gait Posture* 2009;29(1):59–64.
- [21] Goldberg SR, Kepple TM, Stanhope SJ. *In situ* calibration and motion capture transformation optimization improve instrumented treadmill measurements. *J Appl Biomech* 2009;25(4):401–6.
- [22] Werbos PJ. Generalization of backpropagation with application to a recurrent gas market model. *Neural Netw* 1988;1(4):339–56.